Journal of Sol-Gel Science and Technology 30, 35–41, 2004

Thermal Stability of Sol-Gel Derived 6 Mole% CaO-ZrO_2 Ceramics

J.A. MARTÍNEZ, P.C. RIVAS, M.C. CARACOCHE, M.M. CERVERA AND A.M. RODRÍGUEZ
Departamento de Física—Instituto de Física La Plata (CONICET), Facultad de Ciencias Exactas, Universidad Nacional de La Plata, CC67 1900 La Plata, Argentina

R. CARUSO
Departamento de Materiales Cerámicos, FCEIyA-IFIR, Universidad Nacional de Rosario, Av. Pellegrini 250, 2000 Rosario, Argentina

F. SÁNCHEZ-BAJO
Departamento de Electrónica e Ingeniería Electromecánica, Escuela de Ingenierías Industriales, Universidad de Extremadura, Ctra de Elvas s/n, 06071 Badajoz, España

Received April 14, 2003; Accepted February 18, 2004

Abstract. The thermal behavior of the hyperfine interaction at Zr sites on two sol-gel derived 6 mole% CaO-ZrO_2 powders, obtained from the particulate and non-particulate regimes, has been studied by Perturbed Angular Correlations and complementary techniques. The aim was to get experimental support on the thermal stability of the obtained material in order to see the advantages of the different preparation regimes. The results could be interpreted in terms of the different microstructures and nanoscopic configurations exhibited by the resulting powders. After crystallization both powders showed the hyperfine nanoconfigurations of metastable tetragonal zirconia. In the sample obtained following the hydrolysis and the condensation processes via a particulate regime, the undesirable phase transformation towards the monoclinic form of zirconia is inhibited up to higher temperatures.

Keywords: sol-gel regimes, zirconia stabilization, phase content, stabilized tetragonal forms

1. Introduction

Metastable tetragonal and/or cubic zirconias are extensively investigated because of the excellent electrical and structural properties they exhibit. They are used for sensing oxygen, for exchanging ions, for catalytic processes, for improving mechanical properties of materials, etc. Dopants are often used to stabilize the high temperature structures of zirconia at low temperatures. The sol-gel process is widely used to produce zirconia based ceramic materials. This method allows the design of ceramic precursors to obtain high quality ceramics. The key of the design is the control of the hydrolysis rate to avoid the precipitation of hydrous zirconium oxide. Determining factors of this control are the amounts and kinds of solvents, acids and the amount of water available during the process. Zirconium alkoxides behave as good network formers but are also easy to hydrolyze so they need to be chemically modified. It is known that the addition of inorganic acids to the starting solution protonizes alkoxides ligands (OR) affecting the hydrolysis and condensation rates [1]. The ratio of inorganic acid to alkoxide plays an important role during the preparation. In fact, Stöcker et al. [2] have determined that nitric acid to zirconium alkoxide ratios of about 1 induce an acceleration of the hydrolysis, a decrease in the condensation rate and increasing the gel times, being the product a clear polymeric gels.

The reduction of the condensation rates promotes the formation of dense gels. These conditions fall into the so-called non-particulate regime. On the other hand, when a ratio of about 0.1 is used, the hydrolysis and condensation rates are faster and the gel times are less than one minute. The product obtained under this so-called particulate regime is a gelatinous precipitate or colloidal gel with sponge-like microstructure.

Chemical modifications induced by acetic acid are also known [3–5]. It has been established by Hayashi et al. [3] that the acetic acid can replace up to two OR groups attached to Zr. The replacement induces the formation of a stable bidentate chelate compound (with the proposal formula $Zr(OCOCH_3)_2(OR)_2$) that affect the hydrolysis and the condensation reactions. Laaziz et al. [4] confirm that the role of acetic acid as a ligand reduces the strong reactivity of the alkoxide in water. They have reported the formation of crystals of $Zr_9(OPr)_{18}(OAc)_6O_6$ having acetate groups always bridging and propoxy groups bridging or terminals. On the other hand, Peter et al. [5], have assumed the existence of an equilibrium between two different complexes $Zr_2(OPr)_4(OAc)_2$ to give account of their results after the substitution due to the addition of acetic acid.

In the last few years, the gamma-gamma Perturbed Angular Correlation (PAC) technique has been used to determine the internal hyperfine field at Zr lattice sites in order to characterize Zr neighborhoods. PAC, based on the study of the angular distribution of the gamma emissions of radioactive probes, is useful to determine the phase content of a given material as a function of temperature. Taking advantage of the nanoscopic nature of this technique, it is possible to identify different local configurations around Zr in the stabilized tetragonal phase of zirconia. Two different hyperfine quadrupole interactions acting on Zr ions when the tetragonal structure is kept at low temperatures have been found [6, 7]. These distinct interactions are now known as the t-form and t'-form. The first of them corresponds to a slightly asymmetric and almost ordered eightfold-oxygen coordinated tetragonal form and the second to a highly disordered and defective sevenfold-oxygen coordination around Zr. Several studies, using. ^{111}In probes, have been performed to characterize the zirconia phases at different temperatures [see references 8 and 9]. Particular details relative to the measurement of the electric field gradients acting on the probes via the so called spin rotation curves $A_2G_2(t)$ (spin precession as a function of the time elapsed between gamma emissions) were reported elsewhere [see also reference 6].

In this paper, the samples prepared by including nitric acid and acetic acid during the preparation and using Ca dopant are studied. The characteristics of the materials obtained through the particulate and the non-particulate regimes, are discussed at the light of results of several techniques. The thermal behavior of the hyperfine interaction in the resulting materials, using ^{181}Hf as a probe, is monitored by Perturbed Angular Correlation (PAC) experiments.

2. Experimental

2.1. Sample Preparation

A starting alcohol solution of zirconium alkoxide was prepared by mixing 40 ml of zirconium n-propoxide (ZNP) (70% wt in 2-propanol, Alfa 22989) with 51.7 ml of PrOH in N_2 atmosphere and under continuous stirring. The solution was separated in two parts, hereinafter S_1 and S_2, and 6.2 ml of HNO_3 was added to S_1. Calcium acetate (0.91 g) dissolved in 3.5 ml of PrOH and 0.5 ml of HNO_3 was then added to both solutions in order to achieve 6% mole of CaO in the final product. To hydrolyze the solutions, 1.9 ml of acetic acid in 3.3 ml of water (to S_1 solution) and in 5.7 ml of water (to S_2 solution) was added. The molar ratio of HNO_3/ZNP was about 1 for S_1 and of the order of 0.1 for S_2. The final pH of the solutions were 0.5 for S_1 (non-particulate regime) and 5.0 for S_2 (particulate regime). The S_1 solution was clear, yellow and transparent whereas S_2 was a white, opaque and instantaneously gellified solution. Powders were obtained by drying the solutions at 100°C for 48 h in air. The powder obtained from the non-particulate regime (sample Z1) was yellow and the one obtained from the particulate regime (sample Z2) was white.

2.2. Techniques Employed

Scanning electron microscopy (SEM), using a Philips ESEM 2020, was performed on the as-prepared powders. Their specific areas were determined by nitrogen adsorption through the Brunauer-Emmet-Teller (BET) method, using a Micrometrics ASAP 2010 equipment. Differential Thermal Analysis (DTA) and Thermogravimetric Analysis (TGA) were carried out (Shimatzu Series-50 analyzers) on the as-obtained

powders between room temperature and 1200°C at a rate of 10°/min in air. In both cases platinum crucibles were employed and an α-alumina reference was used in DTA. Carbon content of the powders as a function of annealing temperature from 100° to 1000°C were determined in a LECO-200 Carbon and Sulfur Analyzer. Room temperature X-ray diffraction (XRD) was performed on the as-prepared powders and on powders annealed at selected temperatures. Heat treatments were carried out using the same heating rate and atmosphere as in DTA experiment. Data were obtained over the $2\theta = 20°$ to 80° range (steps of 0.02°) and at 5 s per step. A Philips PW1700 diffractometer of 0.0018° instrumental broadening, with graphite monochromator and Cu K_α radiation was used. For Perturbed Angular Correlations (PAC) measurements the powders were encapsulated in air at atmospheric pressure in 0.5 cm^3 sealed quartz tubes. Radioactive ^{181}Hf probes were obtained after irradiation with a thermal neutron flux of about 10^{13} cm^{-2} s^{-1} during approximately one day. PAC spectra were recorded in a two CsF-detectors equipment with a time resolution $\tau_R = 0.9$ ns. Gamma coincidences were stored while the sample was held at a given temperature between RT and 1100°C. To obtain well-defined results, measurements were made over one to two days. The anisotropy of the gamma-gamma angular distribution as a function of the delay time between radiations $A_2G_2(t)$, is calculated from the coincidence spectra and fitted with theoretical models by means of a non-linear least squares fitting procedure. The quadrupole parameters (relative fraction, hyperfine quadrupole frequency, asymmetry parameter, frequency distribution width) depicting the lattice electric field gradients at Zr sites (where ^{181}Hf probes are located) were obtained from the best fits achieved [for details see reference 10].

3. Results

Figure 1 shows the SEM images of both powders. By comparison it is possible to notice the different morphologies. The sample prepared with a molar ratio HNO_3/ZNP $\cong$ 1 (Z1) exhibits a compact microstructure showing planar faces while the one prepared with a ratio HNO_3/ZNP $\cong$ 0.1 (Z2) showed a porous microstructure as proved by BET results which indicate specific area values of 172 and 379 m^2/g for Z1 and Z2 respectively.

Figure 2 displays XRD results. Up to near 400°C the diffractograms seem to correspond to an amorphous-like material. No peaks other than those of zirconia polymorphs were detected at higher temperatures. No typical reflections of the monoclinic phase were observed in either, except in Z1 after the annealing at 1200°C.

Figure 3 shows DTA/TGA results. An endothermic peak centered at approximately 90°C, together with a mass loss of 14% in the TG curve, represents the evaporation of residual adsorbed alcohol and water. Following this change, apparent differences can be observed between the thermal behavior of Z1 and Z2. The first powder exhibits five DTA signals up to 950°C and a mass loss of 38% which finishes at about 500°C. For Z2, only three sharp DTA endothermic processes that end at 490°C are observed, being the mass loss up to 400°C, of about 15%.

The elimination of the organic residues determined by analyzing carbon content as a function of the annealing temperature can be seen in Fig. 4. Carbon losses are observed up to 700°C in Z1 while in Z2 nearly all carbon has been eliminated at 500°C.

Relative to PAC results, two thermal ranges can be roughly determined according to the value and behavior of the fitted interactions. They are represented with open and full symbols in Fig. 5. At lower temperatures, results show that the samples undergone different internal processes. In Z1 three interactions are detected all along this range: $\omega_Q \approx 150$ Mrad/s with $\eta \approx 0.80$ (□), $\omega_Q \approx 210$ Mrad/s with $\eta \approx 0.80$ (○) and $\omega_Q \approx 160$ Mrad/s with $\eta \approx 0.45$ (◇). On the other hand, in Z2 only two of these interactions are observed, those denoted by □ and ○. This last interaction disappears at about 400°C.

At higher temperatures, both samples exhibit the same quadrupole interactions, namely: $\omega_Q \approx 165$ Mrad/s with $\eta \approx 0.07$ (the t-form, ♦ in Fig. 5) and $\omega_Q \approx 150$ Mrad/s with $\eta \approx 0.55$ (the t'-form, ■ in Fig. 5). It is also observed that the characteristic quadrupole interaction of the monoclinic phase ($\omega_Q \approx 120$ Mrad/s and $\eta \approx 0.40$, ◂ in Fig. 5) appears at 950°C in Z1 and at 1080°C in Z2.

4. Discussion and Conclusions

According to BET results which indicate that Z1 has less specific area (172 m^2/g) than Z2 (379 m^2/g) and recalling that the preparation procedure yielded to a clear, yellow and transparent solution for Z1 and a white, opaque and instantaneously gellified solution for Z2, it is clear that Z1 and Z2 were obtained, respectively,

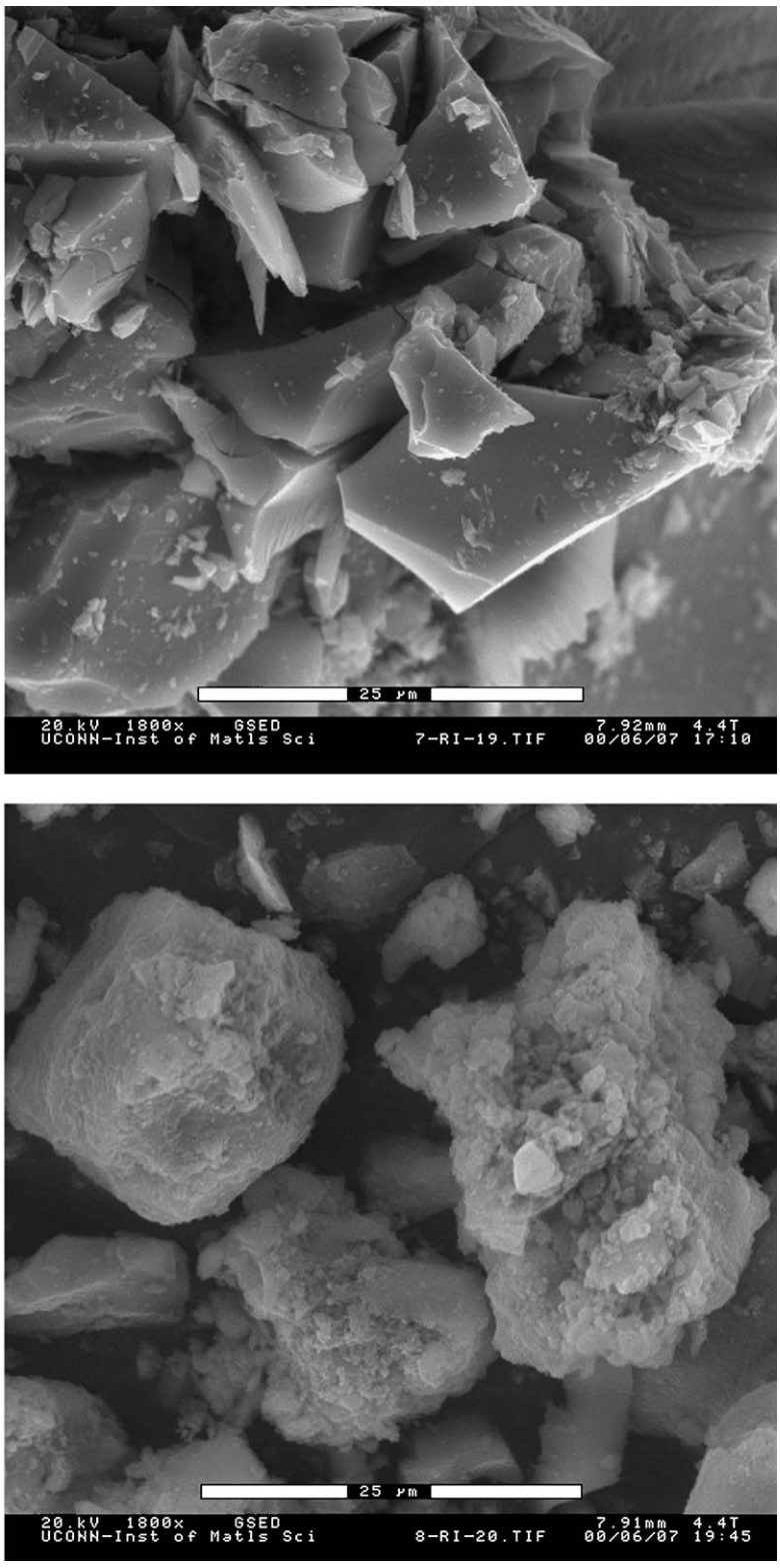

Figure 1. Scanning electromicrograph of the as prepared materials.

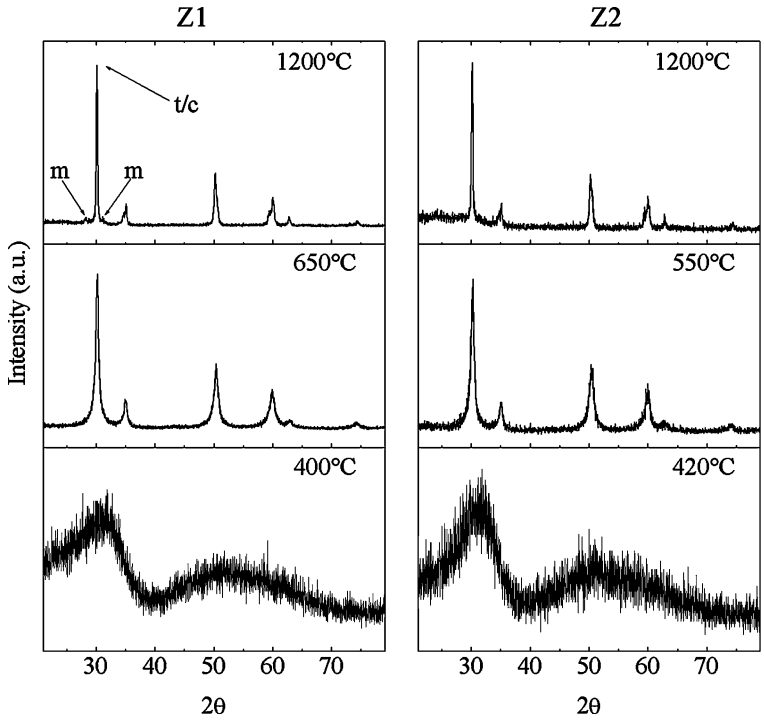

Figure 2. X-ray patterns of Z1 and Z2 taken at room temperature after different thermal treatments. Annealing temperatures are indicated.

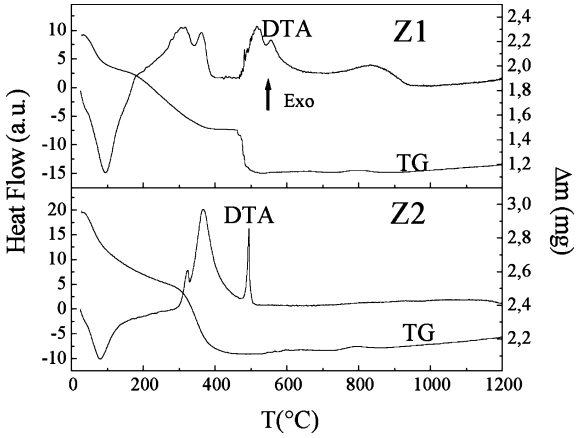

Figure 3. Differential thermal and thermogravimetric analyses performed in air at 10°/min on the as-prepared samples.

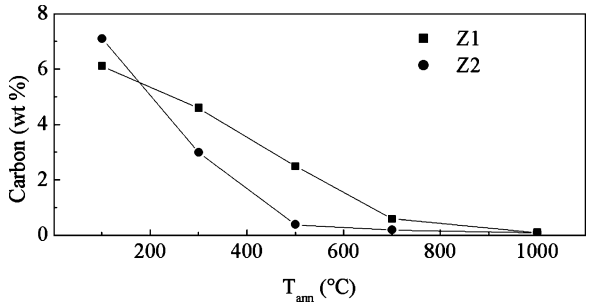

Figure 4. Carbon content of both samples as a function of annealing temperature. Lines joining symbols are just to guide the eye.

via the non-particulate and the particulate regimes described by Stöcker [2]. SEM results give additional support by showing that Z1 appears to have a compact microstructure while Z2 seems to be a sponge-like material. Results of the thermal behavior of the powders obtained under this conditions will be discussed assuming that Z1 has condensed from large polymeric arrangements and Z2 was formed by the condensation of small structures.

In order to guide the discussion about the thermal processes undergone by Z1 and Z2, let us interpret first the carbon content analysis, the DTA/TG diagrams and the X-ray results. As mentioned in the results section, the carbon content of Z1 varies up to 700°C and up to 500°C in Z2. These facts support that the exothermic processes involving mass loss exhibited in the DTA/TG

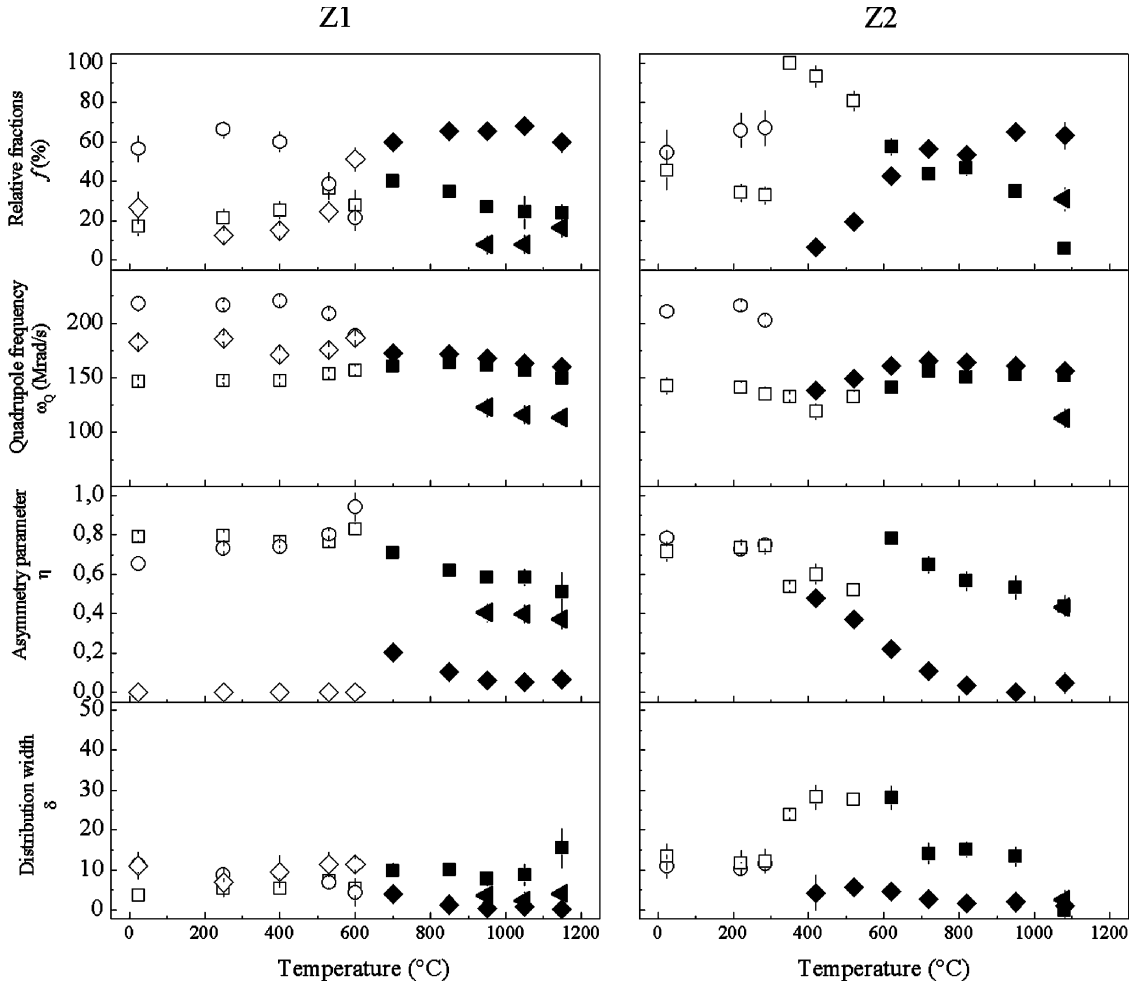

Figure 5. Thermal behavior of the quadrupole hyperfine interactions determined by PAC on the samples Z1 and Z2. ♦ *t*-form, ■ *t′*-form, ◄ *m*-form. Symbols ◇ and □ were used to represent precursors of *t*- and *t′*-forms, respectively. The symbol ○ corresponds to disordered zirconium surroundings containing organic radicals.

curves are associated with the combustion of organic residues. The diagrams show that in Z1 the organic residues are burned in three stages (at 300, 380 and 510°C) while in Z2 only two stages are observed (at 310 and 380°C). So, DTA curves suggest that Zr ions in Z1 are linked to three different organic ligands and in Z2 to two. The burning temperatures indicate that the two organic groups eliminated at lower temperature in both samples are the same. Having Z1 an extra DTA peak and considering that the mass losses are 38% in Z1 and 15% in Z2, it is inferred that during the hydrolysis the replacement of the alkoxide groups by the hydroxyl ones has been less efficient in Z1 than in Z2. On the other hand, X-ray results show that the samples remain amorphous at least up to about 400°C giving additional support to the existence of organic and hydroxyl groups attached to Zr. At about 580°C in Z1 and 490°C in Z2 and once the mass loss almost finished, DTA exothermic signals indicate the crystallization of the samples. X-ray data taken after thermal treatments just over these temperatures confirm the crystallization process into the tetragonal or cubic stabilized phases (see Fig. 2).

Additional information on the structural aspects comes from the hyperfine interaction results. PAC results at lower temperatures indicate that Zr surroundings produce hyperfine interactions similar to those corresponding to higher temperatures. In fact, the frequencies of the interactions denoted by □ and ◇ are close to those of ■ (*t′*-form) and ♦ (*t*-form), respectively, and

their asymmetry parameters tend to the values observed at high temperatures. At lower temperatures, an interaction denoted by ○ is also observed. This interaction disappears at about the same temperature at which the organic groups burn. According to previous works on other ceramic powders obtained via the sol-gel method [11], it is interpreted as an interaction describing disordered Zr surroundings still containing organic radicals.

By analyzing the overall appearance of PAC results under the crystallization temperature, it is possible to infer that both samples have been obtained with a high degree of local structures around Zr which seems to be predecessors of the local structures achieved at higher temperatures. A remarkable fact is that the nonparticulate regime yields a material which includes predecessors of both t- and t'-form of the metastable tetragonal phase and that only the t'-form predecessor is obtained via the particulate regime.

Even when the crystallization process of the samples has been observed by DTA (exothermic peaks at 580°C in Z1 and 490°C in Z2), and the X-ray diffraction pattern (taken after 650°C in Z1 and 550°C in Z2) showed tetragonal or cubic characteristic peaks, the PAC spectra taken at 600°C in both samples support that only the tetragonal forms were achieved. We used PAC to determine the thermal evolution of the phase content in the powders. In Z1, it is clearly observed that after crystallization, the stabilized tetragonal structure of zirconia is mainly the t-form while in Z2 it was possible to determine the growing of the t-form at the expense of the t'-form. It is also noticed that the monoclinic interaction appears once the t-form grows over about 60%. This fact is clearly observed in Z1 at 950°C and at 1080°C in Z2 (see full symbols in Fig. 5). It is clear that the onset of the monoclinic phase occurs from different crystallization products. In Z1 the process exhibits a broad exothermic peak centered at about 850°C and in Z2 no thermal signal is detected. The heat evolved during crystallization, easily measured for Z2 as about 50 J/g, is nearly doubled in the case of Z1 suggesting that in this last sample other processes (maybe dehydroxilation) are taking place during crystallization. Furthermore, from TGA and carbon content data it is possible to infer that from RT to 700°C Z1 loses about 50% of its mass and Z2 28%. Being the carbon losses of about 6–7% for both samples, the differences could be attributed to water, indicating that Z1 contained a greater amount of water than Z2. Gómez et al. [12] have established that dehydroxylation at high temperatures induces the destabilization of the tetragonal phase while at low temperatures it produces point defects which help to stabilize the lattice. On this basis it is possible to suggest that Z1 crystallizes into forms that keep $(OH)^-$ groups up to higher temperatures and that Z2 dehydroxylates before the crystallization.

The present study indicates that to obtain a better stabilized tetragonal zirconia, the chemical procedure followed to obtain Z2 should be recommended or an equivalent procedure avoiding the condensation of large polymeric groups.

The analysis of the results of all the experiments indicates clearly that the stabilization of the tetragonal phase is related to the kind and the amount of precursors which are obtained during the preparation procedure. The presence of the t'-form seems to be an important stabilization factor while the t-form is more labile leading soon to the unwanted degradation of the ceramic via the $t \rightarrow m$ transition.

Acknowledgments

Financial support of Consejo Nacional de Investigaciones Científicas y Técnicas and Comisión de Investigaciones Científicas de la Provincia de Buenos Aires is gratefully acknowledged.

References

1. J. Livage, M. Henry, and C. Sánchez, Prog. Solid State Chem. **18**, 259 (1988).
2. C. Stöcker and A. Baiker, J. Non-Cryst. Solids **223**, 165 (1998).
3. H. Hayashi, H. Suzuki, and S. Kanelo, J. Sol-Gel Sci. Tech. **12**, 87 (1998).
4. I. Laaziz, A. Larbot, C. Guizard, A. Julbe, and L. Cot, Mat. Res. Soc. Symp. **271**, 71 (1992).
5. D. Peter, T.S. Ertel, and H. Bertagnolli, J. Sol-Gel Sci. Tech. **5**, 5 (1995).
6. M.C. Caracoche, P.C. Rivas, M.M. Cervera, R. Caruso, E. Bemavídez, O. de Sanctis, and M.E. Escobar, J. Am. Ceram. Soc. **83**(2), 377 (2000).
7. A.M. Rodríguez, M.C. Caracoche, P.C. Rivas, A.F. Pasquevich, and S.R. Mintzer, J. Am. Ceram. Soc. **84**(1), 188 (2001).
8. N. Mommer, T. Lee, J.A. Gardner, and W.E. Evenson, Phys. Rev. B **61**, 162 (2000).
9. N. Mommer, T. Lee, and J.A. Gardner, J. Mater. Res. **15**, 377 (2000).
10. H. Frauenfelder and R.M. Steffen, in *Alpha-, Beta-, and Gamma-Ray Spectroscopy*, edited by K. Siegbhan (North-Holand Publishing, Amsterdam, 1965), vol. 2, p. 997.
11. R. Caruso, N. Pellegri, O. de Sanctis, M.C. Caracoche, and P.C. Rivas, J. Sol-Gel Sci. Tech. **3**, 241 (1994).
12. R. Gómez, T. López, X. Bokhimi, E. Muñoz, J.L. Boldú, and O. Novarro, J. Sol-Gel Sci. Tech. **11**, 309 (1998).